

# Motion analysis and simulation of a 12-Tetrahedral Walker Robot

Chun Li\*, Hong Nie, Jinbao Chen

State Key Laboratory of Mechanics and Control of Mechanical Structures, Nanjing University of Aeronautics and Astronautics  
Nanjing, 210016, China

Received 6 January 2014, www.tsi.lv

## Abstract

A novel robot mechanism-tetrahedral rolling robot is introduced in the paper. The robot comprises of 26 extension struts and 9 nodes. When the COG of tetrahedron exceeds the stability region, the robot will roll. The structure of the 12-TET robot is described. Designing method of the robot is given, and it is proved correct and feasible through simulation. Kinematic models in different motion phases are analysed in the paper, and the rolling critical condition is formulated. The effectiveness of the method is testified through simulation. The study of the paper will provide important reference for the dynamic analysis, optimization design and control of the tetrahedral rolling robot.

*Keywords:* Variable tetrahedron robot, Gait planning, Motion analysis

## 1 Introduction

A cutting-edge technology is Tetrahedral Robotics (TR), which involves active trusses made up of extensible structural members (struts) and interconnections (nodes) arranged in a tetrahedral mesh [1]. This conception is originally presented by Hamlin and Sanderson. The movement of a tetrahedral robot is realized through length change of the truss, and it is a novel mechanism with multi-DOF and multi-loop [2]. The robot moves by changing the lengths of several struts, which changes the location of the centre of gravity (COG). If the centre of gravity (COG) of the robot exceeds the stable region, it may cause the robot to “tumble”. The number of tetrahedra, or TETs, is an indicator of the complexity of a TR robot and the behaviours and shapes it can take on [3].

Tetrahedral Walker Robots provide greater mobility than conventional wheeled or track robots. This includes the abilities to [4]:

- 1) Traverse terrain more rugged in terms of slope, roughness, and obstacle size.
- 2) Conform to virtually any terrain.
- 3) Avoid falling down or getting stuck permanently.
- 4) Be easily maintained due to its modularity.
- 5) Avoid failure through compensatory gait (limp).

Tetrahedral Walker Robots architecture is being developed at NASA Goddard Space Flight Center (GSFC) for Lunar or Martian exploration [5]. The current line of work at GSFC on TR began in 2004 with the development of the 1-TET, a one-tetrahedron reconfigurable truss that demonstrated basic movement

and control of a determined system [6]. The second-generation 12-TET was deficient in a number of ways because of its weight. The third-generation TR 12-TET is so complex that it cannot move, and now the control method is in research [7, 8].

## 2 Mechanism design of tetrahedral walker robot

The mechanism sketch map of a variable 12-tetrahedral robot is shown in Figure 1.

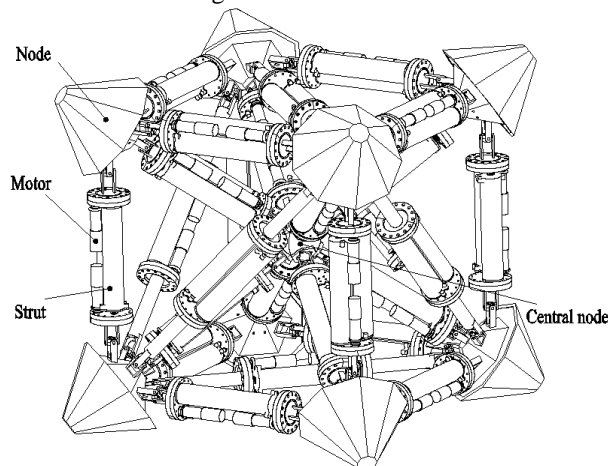


FIGURE 1 The configuration of a variable 12-tetrahedral robot

This 12-TET robot has an interior node for a payload and more continuous motion. The tetrahedral framework acts as a simple skeletal muscular structure [5]. The 12-TET is a mechanism with 9 nodes, and 26 struts which can look a lot like a box with a central node connected to each corner by a strut. There is a strut along each edge of the box and a diagonal strut on each face.

\* Corresponding author e-mail: chlihb@163.com

The geometry of the strut is a back-to-back double sided geometry expanding in two directions, improving the extension ratio with fewer segments and reducing crowding at the nodes. For actuation we have developed a

system of nested screws Figure 2 within an exoskeleton Figure 3, which has a greater extension ratio than we believe has previously been achieved.

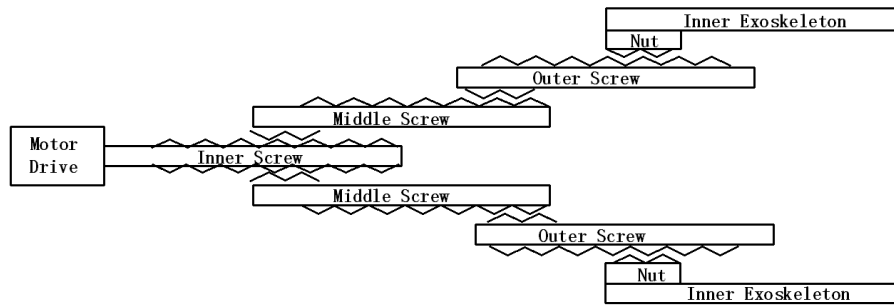


FIGURE 2 Screw design

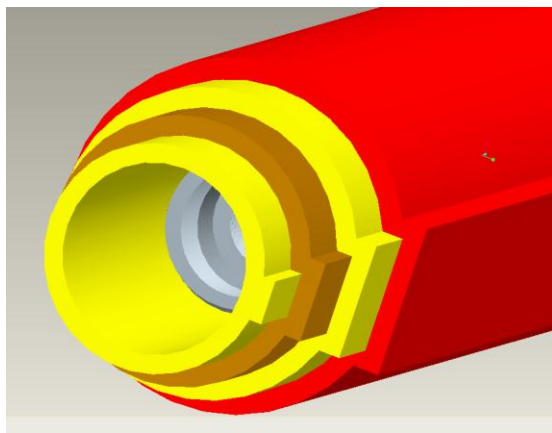


FIGURE 3 Exoskeleton design

Exoskeleton cannot spin, which keeps the last nut from spinning, which makes the system progress linearly when the motor spins the inner screw.

**3 Kinematic models analysis**

The variable 12-tetrahedral robot’s movement is defined from the base configuration of the 12-TET shown in Figure 4a. The structure has 4 nodes that connect 7 struts (node 1, 3, 5 and 7), 4 nodes that connect 4 struts (node 2, 4, 6 and 8) and a centre node (node C)

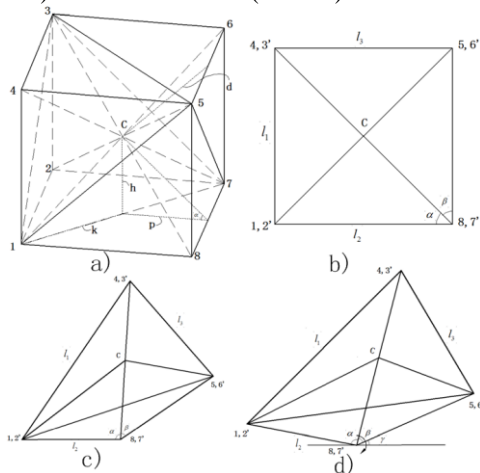


FIGURE 4 The base configuration of a variable 12-tetrahedral robot

**3.1 TUMBLING MOVEMENT**

We assume that the mass of the struts are negligible compared to that of the nodes, and each node’s mass of the variable 12-TET robot is equable. The variable 12-TET robot has different kinds of motion pattern, and one pattern that included two movements is chosen to analyse: Tumbling occurs over one of the four sides of the base (Square 1278). Supposing that robot would topple over the 78 strut. In the process of movement, node 3, 4, 7, 8 and node C is always located in the same Plane. For the first movement, the struts between Node a and Node b ( $L_{ab}$ ) will be extending with the following length constraints (L is the initial length for the struts):

$$L_{14} = L_{23} = l_1, L_{13} = \sqrt{L^2 + l_1^2}, L_{18} = L_{27} = l_2,$$

$$L_{17} = \sqrt{L^2 + l_2^2}, L_{45} = L_{36} = l_3, L_{35} = \sqrt{L^2 + l_3^2},$$

$$L_{1C} = L_{2C} = \sqrt{h^2 + k^2}, L_{5C} = L_{6C} = \sqrt{d^2 + \frac{L^2}{2}},$$

$$L_{15} = \sqrt{L^2 + l_2^2 - 2Ll_2 \cos(\alpha + \beta)},$$

$$\alpha = \arccos\left(\frac{2L^2 + l_2^2 - l_1^2}{2\sqrt{2}Ll_2}\right), \beta = \arccos\left(\frac{3L^2 - l_3^2}{2\sqrt{2}L^2}\right), \quad (1)$$

$$h = \frac{\sqrt{2}}{2} L \sin \alpha, p = \frac{\sqrt{2}}{2} L \cos \alpha,$$

$$k = \sqrt{\left(\frac{L}{2}\right)^2 + (L - p)^2}, d = \sqrt{\frac{3}{2}L^2 - \sqrt{2}L^2 \cos \beta}.$$

The rest of the struts do not change their lengths.

Now we consider the geometry of the robot and find the conditions under which the robot tumbles. We will show that tumbling occurs at certain ratios of the sides of the robot base. We should therefore change its dimensions accordingly. Once the torques about the 78 strut equals each other, the robot is going to topple.  $\alpha$  is

the angle that rectangle 4378 relative to its initial position. The toppling critical condition is:

$$2l_2 + 2\sqrt{2}l_o \cos \alpha + \frac{\sqrt{2}}{2}l_0 \cos \alpha \geq -2l_0 \cos(\alpha + \beta),$$

$$\cos(\alpha + \beta) \geq \frac{5l_1^2 - 13l_2^2 - 10L^2}{8Ll_2} \quad (2)$$

### 3.2 KINEMATIC MODEL ANALYSIS BEFORE TOPPLING

#### 3.2.1 Jacobi [J] and Hessian [H]

According to the mechanism characteristic and motion pattern of the variable 12-tetrahedral robot, the coordinates are established as Figure 5.

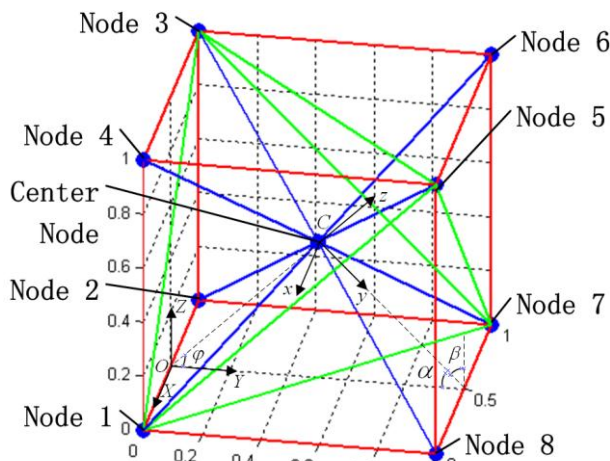


FIGURE 5 Coordinates of the variable 12-tetrahedral robot

Inertial frame (O-XYZ) and moving coordinates (C-xyz) is shown. Mid-point (O) of  $L_{12}$  for origin of inertial frame (O-XYZ), Axis X is perpendicular with plane 1234, Axis Y is superposed on line 12, and Axis Z can be deduced by the right hand rule. Centre node (C) for origin of moving coordinates (C-xyz), Axis z is perpendicular with  $\Delta 8C7$ , Axis x is superposed on midline of  $\Delta 8C7$ , and Axis y can be deduced by the right hand rule. Thus it can be seen, angle  $\alpha$  between z and Z is the dihedral angle between plane 8C7 and plane 1278.

An arbitrary vector ( $R'$ ) in the moving coordinates (C-xyz) transformation to inertial frame (O-XYZ) given by:

$$R = [T]R' + PABC, \quad (3)$$

wherein

$$T = \begin{bmatrix} 1 & 0 & 0 \\ 0 & \cos \alpha & \sin \alpha \\ 0 & -\sin \alpha & \cos \alpha \end{bmatrix}, \quad (4)$$

$$P = [0 \ Y_c \ Z_c]^T, \quad (5)$$

in which  $Y_c = l_2 - \frac{\sqrt{2}}{2}L \cos \alpha$  and  $Z_c = \frac{\sqrt{2}}{2}L \sin \alpha$ .

Supposing that the position and the pose of component  $i$ 's centre of the variable 12-tetrahedral robot is expressed as  $U_i, \Phi_i$ , and  $U_i, \Phi_i$  is the non-linear function of joint variable  $l, l = (l_1, l_2, l_3)^T$ . The equation is

$$U_i = f_1(l_1, l_2, l_3) \quad (6)$$

$$\Phi_i = f_2(l_1, l_2, l_3) \quad (7)$$

The first differential coefficient of them are the velocity  $v_i$  and angle velocity  $\omega_i$  of component  $i$ . The equation is

$$v_i = \dot{U}_i = \begin{bmatrix} \frac{\partial f_1}{\partial l_1} & \frac{\partial f_1}{\partial l_2} & \frac{\partial f_1}{\partial l_3} \end{bmatrix} \begin{bmatrix} \dot{l}_1 & \dot{l}_2 & \dot{l}_3 \end{bmatrix}^T = J_{T,i} \dot{l}, \quad (8)$$

$$\omega_i = \dot{\Phi}_i = \begin{bmatrix} \frac{\partial f_2}{\partial l_1} & \frac{\partial f_2}{\partial l_2} & \frac{\partial f_2}{\partial l_3} \end{bmatrix} \begin{bmatrix} \dot{l}_1 & \dot{l}_2 & \dot{l}_3 \end{bmatrix}^T = J_{R,i} \dot{l}. \quad (9)$$

The second differential coefficient of them are the acceleration  $a_i$  and  $\varepsilon_i$  of component  $i$ . The equation is

$$a_i = \ddot{U}_i = \dot{J}_{T,i} \dot{l} + J_{T,i} \ddot{l} = H_{T,i} \dot{l} + J_{T,i} \ddot{l}, \quad (10)$$

$$\varepsilon_i = \ddot{\Phi}_i = \dot{J}_{R,i} \dot{l} + J_{R,i} \ddot{l} = H_{R,i} \dot{l} + J_{R,i} \ddot{l}. \quad (11)$$

$J_{T,i}, H_{T,i}$  are the translational Jacobi matrix and Hessian matrix,  $J_{R,i}, H_{R,i}$  are the rotational matrix.

#### 3.2.2 Jacobi [J] and Hessian [H] of nodes

Take centre node (C) for example, the position and the pose of C's centroid is:

$$U_C = P = \begin{bmatrix} 0 \\ Y_C \\ Z_C \end{bmatrix} = \begin{bmatrix} 0 \\ l_2 - \frac{\sqrt{2}}{2} L \cos \alpha \\ \frac{\sqrt{2}}{2} L \sin \alpha \end{bmatrix}, \quad (12)$$

$$\Phi_C = \begin{bmatrix} \varphi \\ 0 \\ 0 \end{bmatrix} = \begin{bmatrix} \arctan\left(\frac{\sqrt{2} L \sin \alpha}{2l_2 - \sqrt{2} L \cos \alpha}\right) \\ 0 \\ 0 \end{bmatrix}, \quad (13)$$

where  $\alpha = \arccos\left(\frac{2L^2 + l_2^2 - l_1^2}{2\sqrt{2}Ll_2}\right)$ .

According to formula (8) ~ (11), the velocity  $v_C$  and angle velocity  $\omega_C$  of node C is:

$$v_C = \dot{U}_C = J_{T,C} \dot{l} = J_{T,C} (l_1, l_2, l_3)^T, \quad (14)$$

$$\omega_C = \dot{\Phi}_C = J_{R,C} \dot{l} = J_{R,C} (l_1, l_2, l_3)^T \quad (15)$$

the acceleration  $a_C$  and  $\varepsilon_C$

$$a_C = \ddot{U}_C = \dot{J}_{T,C} \dot{l} + J_{T,C} \ddot{l} = H_{T,C} \dot{l} + J_{T,C} \ddot{l}, \quad (16)$$

$$\varepsilon_C = \ddot{\Phi}_C = \dot{J}_{R,C} \dot{l} + J_{R,C} \ddot{l} = H_{R,C} \dot{l} + J_{R,C} \ddot{l}. \quad (17)$$

Similarly, we can obtain other nodes' J, H and velocity, acceleration.

### 3.2.3 Jacobi [J] and Hessian [H] of struts

The geometry of the struts is a back-to-back double sided geometry expanding in two directions, and the centroid in the geometric centre of struts. Take strut C5 for example; the position and the pose of strut C5's centroid in the moving coordinate is:

$$U_{C5} = \begin{bmatrix} \frac{x_5}{2} \\ \frac{y_5}{2} \\ \frac{z_5}{2} \end{bmatrix}, \quad \Phi_{C5} = \begin{bmatrix} \delta \\ 0 \\ 0 \end{bmatrix}, \quad (18)$$

where  $\delta = \arccos\left(\frac{l_3^2 - L^2}{2Ll_3}\right)$ ,  $x_5 = \frac{L}{2}$ ,  $y_5 = \frac{l_3^2 - L^2}{2\sqrt{2}L}$ , and  $z_5 = \frac{\sqrt{4l_3^2L - l_3^4 - L^4}}{2\sqrt{2}L}$ .

According to formula (3), the position and the pose of strut C5's centroid in the inertial frame (O-XYZ) is:

$$U_{C5} = [T]U'_{C5} + P, \quad \Phi_{C5} = [T]\Phi'_{C5} + P \quad (19)$$

The velocity  $v_{C5}$  and angle velocity  $\omega_{C5}$  of strut C5 is:

$$v_{C5} = \dot{U}_{C5} = J_{T,C5} (l_1, l_2, l_3)^T, \quad (20)$$

$$\omega_{C5} = \dot{\Phi}_{C5} = J_{R,C5} (l_1, l_2, l_3)^T. \quad (21)$$

The acceleration  $a_{C5}$  and  $\varepsilon_{C5}$

$$a_{C5} = \ddot{U}_{C5} = \dot{J}_{T,C5} \dot{l} + J_{T,C5} \ddot{l} = H_{T,C5} \dot{l} + J_{T,C5} \ddot{l} \quad (22)$$

$$\varepsilon_{C5} = \ddot{\Phi}_{C5} = \dot{J}_{R,C5} \dot{l} + J_{R,C5} \ddot{l} = H_{R,C5} \dot{l} + J_{R,C5} \ddot{l} \quad (23)$$

Similarly, we can obtain other struts' J, H and velocity, acceleration.

### 3.3 FALLING PHASE

The process of beginning the fall of the 12-TET robot is shown in fig.2. Supposing that the vector of strut 87 is:

$$\vec{u}_{87} = (u_x, u_y, u_z)^T. \quad (24)$$

The falling path of robot is expressed

$$\vec{v} = [R_{\beta,\gamma}] [R_{-\gamma,x}] [R_{\phi,z}] [R_{\gamma,x}] [R_{-\beta,\gamma}] \vec{v}_0 = [R_{\phi,u}] \vec{v}_0 \quad (25)$$

Rotational matrix

$$[R_{\phi,u}] = \begin{bmatrix} u_x^2 V \phi + \cos \phi & u_x u_y V \phi - u_z \sin \phi & u_x u_z V \phi + u_y \sin \phi \\ u_x u_y V \phi + u_z \sin \phi & u_y^2 V \phi + \cos \phi & u_y u_z V \phi - u_x \sin \phi \\ u_x u_z V \phi - u_y \sin \phi & u_y u_z V \phi + u_x \sin \phi & u_z^2 V \phi + \cos \phi \end{bmatrix} \quad (26)$$

where  $V \phi = 1 - \cos \phi$ ,  $\sin \gamma = u_y$ ,  $\sin \beta = \frac{u_x}{\sqrt{u_x^2 + u_z^2}}$ ,

$\cos \gamma = \sqrt{u_x^2 + u_z^2}$ ,  $\cos \beta = \frac{u_z}{\sqrt{u_x^2 + u_y^2}}$ ,  $\cos \gamma \sin \beta = u_x$ ,

and  $\cos \gamma \cos \beta = u_z$ ,  $\phi$  is the roll angle of the robot.

Different walking paths can be planned through choosing different roll axis. Trajectory of the variable 12-

tetrahedral robot is shown in Figure 6. It is seen that the tetrahedral rolling robot could change its walking direction anytime, so it has great agility

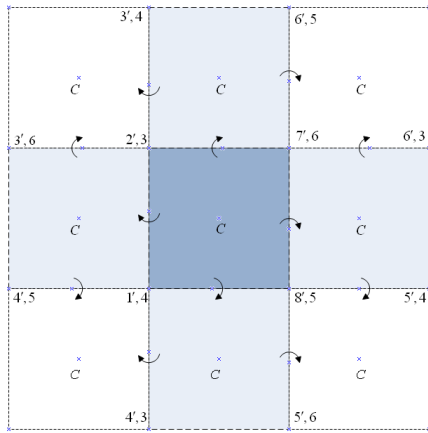


FIGURE 5 Trajectory of the variable 12-tetrahedral robot

**4 Simulation**

The simulation model is built for validating the effectiveness of the kinematic analysis method. The

parameter of the model is as follows: original length of strut  $L=1000\text{mm}$ .

We simulate the theoretical relations within MATLAB shown in Figure 6. This movement (Figure 7 a, b, c) moves the COG of the structure outside of the base and makes the robot tumble (Figure 7 d). The second movement (Figure 7 e, f) that completes the motion pattern involves the contraction of the same struts involved in the first movement. The contraction of the struts follows the same constraints of the first movement as well. Repeating this sequence of movement makes the robot move in a tumbling way.

The Adams simulation 12-TET robot is shown in Figure 8. It shows that the robot can realize the rolling motion according to the planned path, and then relapse. It indicates that the design method is feasible. The next movement can choose different roll axis and motion parameter; including direction, step length, and height. These can all be set neatly.

In the paper, the velocity of the extension strut is slow, and the dynamic effect is small. When the velocity increases, the dynamic effect will become greater. The next work will study this problem deeper.

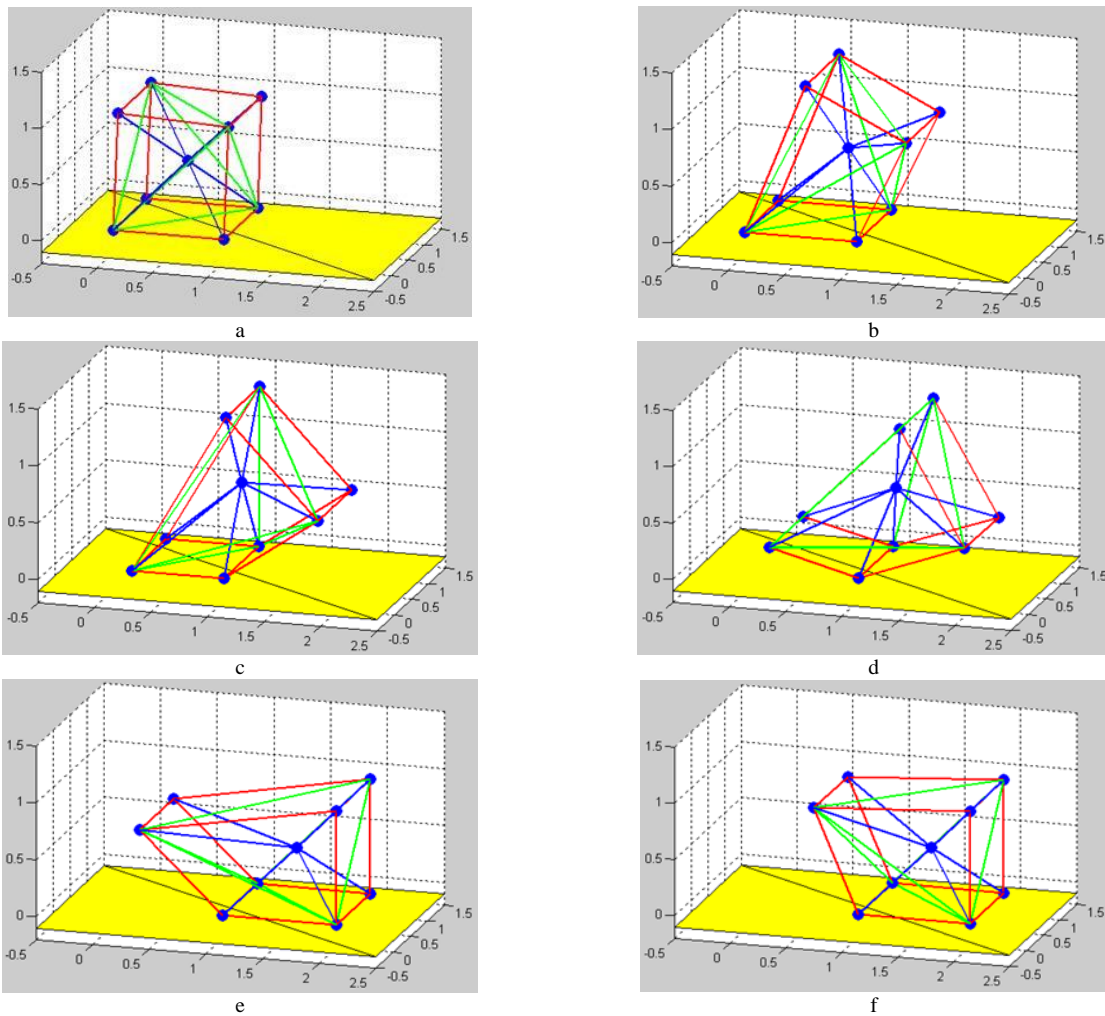


FIGURE 7 Rolling gait

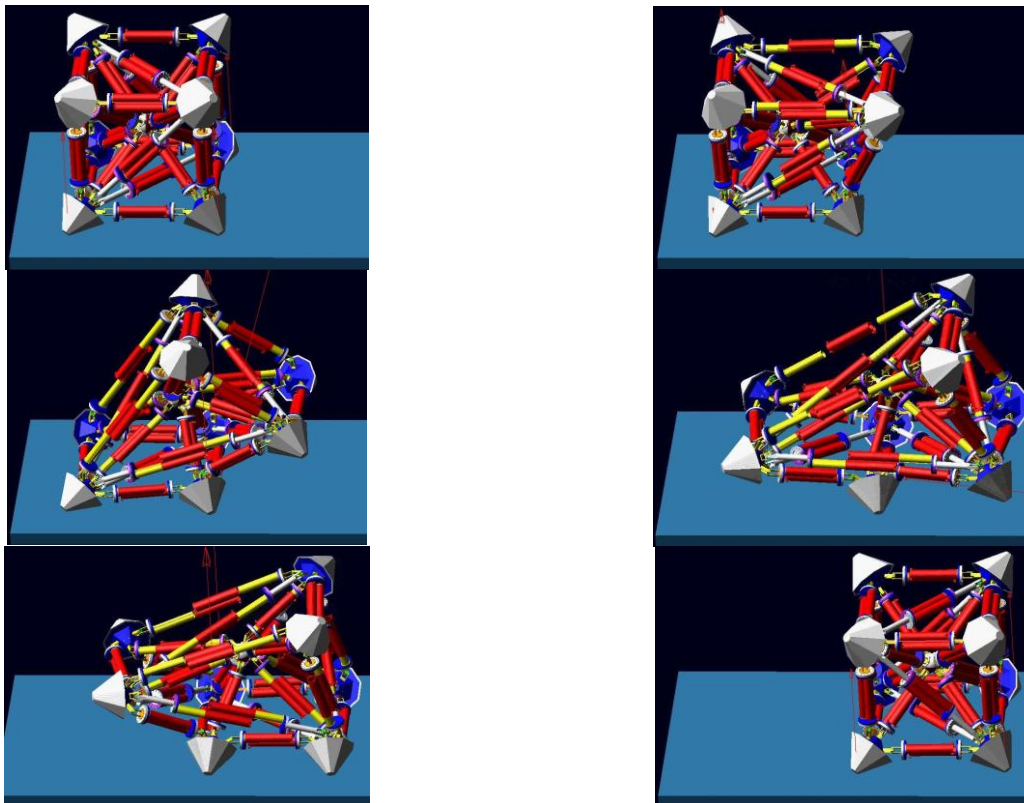


FIGURE 8 The Adams simulation 12-TET robot

**References**

[1] Curtis S, Brandt M, Bowers G 2007 Tetrahedral robotics for space exploration *IEEE Aerospace and Electronic Systems Magazine* 22(6) 22-30

[2] Miguel Abrahantes, Aaron Silver, Luke Wendt 2007 Gait Design and Modeling of a 12-Tetrahedron Walker Robot *39th Southeastern Symposium on System Theory* 10(2) 39-43

[3] Maziar Izadi, M J Mahjoob, Mohammad Soheilypour 2010 A Motion Planning for Toppling-Motion of a TET Walker *The 2nd International Conference on Computer and Automation Engineering* 8(4) 34-9

[4] Abrahantes M, Smits C 2012 Implementation and control of a reconfigurable 8-Tetrahedral robot *Electro/Information Technology (EIT), 2012 IEEE International Conference on* 6-8 May 2012 1-5

[5] Wan Ding, Sung-Chan Kim, Yan-An Yao 2012 A pneumatic cylinder driving polyhedron mobile mechanism *Frontiers of Mechanical Engineering* 7(1) 55-65

[6] M Abrahantes, D Littio, A Silver, L Wendt 2008 Modeling and Gait Design of a 4-Tetrahedron Walker Robot *System Theory, 2008. SSST 2008. 40th Southeastern Symposium on* 16-18 March 2008 269-73

[7] P E Clark, M L Rilee, S A Curtis 2004 BEES for ANTS: Space Mission Application for the Autonomous Nano Technology Swarm *AIAA 1st Intelligent Systems Technical Conference* 20-22 September 2004 1-12

[8] Abrahantes, M, Nelson L, Doorn P 2010 Modeling and Gait Design of a 6-Tetrahedron Walker Robot *System Theory (SSST) 2010 42nd Southeastern Symposium on* 5 248-52

[9] Zhang Lige, Bi Shusheng, Peng Zhaoqin 2011 Motion analysis and simulation of tetrahedral rolling robot *Journal of Beijing University of Aeronautics and Astronautics* 37(4) 415-20

<b>Authors</b>	
	<p><b>Chun Li, born in February, 1986, Nanjing, Jiangsu Province, P.R. China</b></p> <p><b>Current position, grades:</b> Ph.D candidate of School of Machinery theory and design, Nanjing University of Aeronautics and Astronautics, China.</p> <p><b>University studies:</b> B.Sc. in Aircraft Design and Engineering from Northwestern Polytechnical University in China (2006-2010).</p> <p><b>Scientific interest:</b> a 12-tetrahedral rolling robot</p> <p><b>Publications:</b> 3 patents.</p> <p><b>Experience:</b> 1 scientific research project.</p>
	<p><b>Hong Nie, born in January, 1960, Anhui Province, P.R. China</b></p> <p><b>Current position, grades:</b> Professor of School of Aircraft Design, Nanjing University of Aeronautics and Astronautics, China.</p> <p><b>University studies:</b> Ph.D. in Aircraft Design from Northwestern Polytechnical University in China.</p> <p><b>Scientific interest:</b> rolling robot, gear design</p> <p><b>Publications:</b> 80papers, 30 patents.</p> <p><b>Experience:</b> teaching experience of 23 years, 10 scientific research projects.</p>
	<p><b>Jinbao Chen, born in June, 1980, Nanjing, Jiangsu Province, P.R. China</b></p> <p><b>Current position, grades:</b> Associate Professor of School of Nanjing University of Aeronautics and Astronautics, China.</p> <p><b>University studies:</b> Ph.D. in Aircraft Design from Nanjing University of Aeronautics and Astronautics in China (2005-2008).</p> <p><b>Scientific interest:</b> gear design, soft landing of lunar</p> <p><b>Publications:</b> 20papers.</p> <p><b>Experience:</b> teaching experience of 4 years, 6 scientific research projects.</p>